

It's a super deal – train recurrent network on *noisy* data and get *smooth* prediction free

Boris Rubinstein,
Stowers Institute for Medical Research
1000 50th St., Kansas City, MO 64110, U.S.A.

May 2, 2023

Abstract

Recent researches demonstrate that prediction of time series by predictive recurrent neural networks based on the noisy input generates a *smooth* anticipated trajectory. We examine influence of the noise component in both the training data sets and the input sequences on network prediction quality. We propose and discuss an explanation of the observed noise compression in the predictive process. We also discuss importance of this property of recurrent networks in the neuroscience context for the evolution of living organisms.

1 Introduction

Recurrent neural networks (RNNs) due to their ability to process ordered sequences of data have found applications in many fields of science, engineering and humanities. RNNs represent the most important elements of predictive recurrent networks (PRN). One of the PRN applications is time series prediction used in analysis of business and financial data, weather forecast *etc.* It is believed that animal brains also use some kind of PRNs to predict moving object trajectories. Trajectory prediction based on incomplete or noisy data is one of the most amazing features of organism brains that allows living creatures to survive in complex and usually unfriendly environment.

What does happen when a smooth trajectory is perturbed by an external noise of specific statistics, *e.g.*, white noise? How would PRN extrapolate the input of such noisy time series? Generally speaking, when a noisy signal is used as an input to a PRN it is expected that a trained network would be able to extrapolate the *noisy* time series. It appears that the extrapolated trajectory is not noisy – filtering of the noisy perturbation of the Lorenz attractor dynamics is reported in recurrent multi-layer perception network – the reconstructed signals are "reasonably close to the noise-free signal and the iterated predictions are smoother in comparison to the noisy signals" [1]. This observation leads to the following question – given a smooth deterministic function with added noise component as a PRN input will the trajectory anticipated by the network be noisy or smooth? A short note [2] considers LSTM network [3] with small number (128) of neurons trained on the Mackey-Glass time series with added noise. It appears that with the increase of the noise level PRN behavior depends more on its own dynamics than on the input data. On the contrary, the training using the noiseless input produces PRN with very high sensitivity to small perturbations.

The author of this manuscript reported earlier that PRN trained on segments of *noisy* trajectory and being fed a segment of such trajectory produces a *smooth* extrapolating curve and this effect is independent of the PRN architecture, size and depth [4,5]. It was shown that PRNs do not *filter out* the noise component of the input sequence but somehow predicts a smooth curve that is quite close to the actual noise-free dynamics. The effect is observed for different training algorithms and prediction procedures [4–6]. In this manuscript we investigate an influence of the noise amplitude in the training data sets and input sequences on the network prediction of actual trajectory. We also discuss a possible reason for the observed PRN ability to generate a smooth time series and argue that it is related to the PRN training procedure and enhanced by the predictive

algorithms. In this manuscript the term "smooth" for description of the predicted trajectories means that *the deviation from the actual trajectory is negligible compared to the noise amplitude of the input sequence fed into the network.*

2 Recurrent network training and predictive algorithms

A typical PRN is designed to use an input sequence $\mathbf{X} = \{\mathbf{x}_i\}$, $1 \leq i \leq m$ of m elements \mathbf{x}_i that represents a segment of the time series in order to generate a predicted sequence of p elements \mathbf{x}_{m+j} , $1 \leq j \leq p$ determining the consecutive part of the same time series, so that the elements of both the input and predicted sequences should have similar structure (numerical vectors, words, symbols, images, musical notes *etc.*).

2.1 Network training

To perform this task PRN should be first trained using a training set consisting of sequences of fixed or variable length m , each sequence $\mathbf{X} = \{\mathbf{x}_i\}$ is accompanied by either a single next element \mathbf{x}_{m+1} for "seq-to-one" PRNs [4, 5] or a sequence of elements $\{\mathbf{x}_i\}$, $m + 1 \leq i \leq m + l$ for "seq-to-seq" network [6]. In this manuscript we focus on "seq-to-one" RNNs. In this case for each training set \mathbf{X}^k PRN produces a prediction $\bar{\mathbf{x}}_{m+1}^k$ that compared to the actual values \mathbf{x}_{m+1}^k . The network parameters are fitted to minimize the mean square difference (a training error E_{tr}) after N training rounds

$$E_{tr} = (1/N) \sum_{k=1}^N |\bar{\mathbf{x}}_{m+1}^k - \mathbf{x}_{m+1}^k|^2.$$

Once the network is trained it can be used to generate several consecutive values $\bar{\mathbf{x}}_{m+j}$, $1 \leq j \leq p$.

The mode of prediction for "seq-to-one" PRNs is the following. An inner state (an activation level) of the network n neurons is described by a n -dimensional vector \mathbf{s} . Its discrete dynamics is usually governed by a vector map

$$\mathbf{s}_i = \mathbf{F}(\mathbf{x}_i, \mathbf{s}_{i-1}, \mathbf{P}), \quad (1)$$

where \mathbf{F} determines the network architecture and \mathbf{P} embraces the network trainable parameters. Assuming these parameters fixed for the trained network we drop this argument below. This algorithm describes the neurons having no memory so that the current state \mathbf{s}_i of the network depends only on the current input signal \mathbf{x}_i and the previous RNN state \mathbf{s}_{i-1} while the parameter values are fixed during the prediction process. The last state \mathbf{s}_m of the network is transformed linearly to predict a single point $\bar{\mathbf{x}}_{m+1}$

$$\bar{\mathbf{x}}_{m+1} = \mathbf{L}(\mathbf{s}_m) = \mathbf{W} \cdot \mathbf{s}_m + \mathbf{b}, \quad (2)$$

where \mathbf{W} is a matrix and \mathbf{b} is a bias vector both have trainable parameters.

2.2 Prediction algorithms

When the network is trained on the sequences of the fixed length the standard predictive algorithm uses a "moving window" (MW) recursion. One starts with a sequence \mathbf{X}^1 of length m supplied as an input to the network; it leads to generation of a predicted point $\bar{\mathbf{x}}_{m+1}$. The next input sequence \mathbf{X}^2 is produced by dropping the first point of \mathbf{X}^1 and adding the predicted point $\bar{\mathbf{x}}_{m+1}$ to the result. This sequence is used as a new input leading to generation of $\bar{\mathbf{x}}_{m+2}$ and the next input \mathbf{X}^3 is formed. Thus at k -th predictive step the input \mathbf{X}^k to PRN is formed by adding to the original input \mathbf{X}^1 all previously $k - 1$ predicted points and shifting the window by $k - 1$ steps forward. The recursive procedure is repeated p times to produce a sequence of p points $\bar{\mathbf{x}}_{m+j}$, $1 \leq j \leq p$ approximating the sequence $\{\mathbf{x}_i\}$ for $m + 1 \leq i \leq m + p$. It should be noted that this approach is used to produce all the figures in the next section.

For network training with sequences of the variable length (not larger than some M) the MW predictive algorithm can be modified into the "expanding window" (EW) version. After each predictive round the newly generated point is added to the original input sequence, so that after the k -th prediction round the length of the input sequence \mathbf{X}^k is $m + k$, where m denotes the size of the initial input sequence and $m + k \leq M$.

The main reason of EW algorithm application is that a gradual increase of the input length usually leads to better prediction quality and it also produces smoother anticipated trajectories.

It should be underlined that both above algorithms require some memory unit to store the input sequence values and thus they perform their task *non-autonomously*. From the biological perspective the presence of such a unit requires additional resources that might not be available. The author recently suggested [4, 5] a memoryless (ML) algorithm generating smooth trajectories that coincide with high accuracy with the trajectories predicted by the traditional algorithms. This *autonomous* algorithm can be applied for any (even untrained) predictive network. In Appendix we show that ML algorithm is just a "compression" of the regular EW procedure.

2.3 Training set and prediction input sequences

As PRNs process discrete data sets (time series) and we are interested in the noise influence on the network prediction quality we have to define sequences that describe smooth trajectories with (significant) noise components added. Introduce a smooth continuous vector function $\mathbf{f}(t)$ of the scalar argument representing an actual trajectory in the phase space. An apparent trajectory fed into a network is defined by $\mathbf{g}(t, a) = \mathbf{f}(t) + a\boldsymbol{\xi}(t)$ with the noise component $\boldsymbol{\xi}(t)$ of specific statistics (say, white noise) and amplitude a . We assume that the noise average vanishes $\langle \boldsymbol{\xi}(t) \rangle = 0$. Define a fixed or variable time step Δt and generate a sequence $\mathbf{G}(a) = \{\mathbf{g}_j(a)\}$ where $\mathbf{g}_j(a) = \mathbf{g}(t_0 + j\Delta t, a) = \mathbf{f}_j + a\boldsymbol{\xi}_j$. The training sets are constructed from the sequence $\mathbf{G}(a_0)$ and the input sets used for the prediction by a trained PRN represent the sequence $\mathbf{G}(a_i)$ where $0 \leq a_0, a_i \leq a_m$. The maximal noise amplitude a_m assumed to be comparable to the characteristic range of values of the smooth function $\mathbf{f}(t)$.

3 RNN training and performance

The network training with noisy input sequences requires multiple data sets that have the same actual smooth trajectory $\mathbf{f}(t)$ or sequence \mathbf{f}_j and perturbations $a_0\boldsymbol{\xi}(t)$ or $a_0\boldsymbol{\xi}_j$.

3.1 Network architecture and training data sets

The PRNs with a single recurrent basic or LSTM layer [3] have a small number $n = 20$ of neurons. For each trajectory and given noise amplitude $a_0 = 0, 0.15, 0.4, 0.75$ the training set is constructed by generating 6000 segments of variable length ($5 \leq m \leq 50$).

We considered two qualitatively different types of trajectories. In order to save computational resources one can use a periodic function $\mathbf{f}(t)$ with hundreds of periods to generate a discrete sequence $\mathbf{f}_j = \mathbf{f}(t_j)$ and add to each point of this sequence $a_0\boldsymbol{\xi}_j$ where $\boldsymbol{\xi}_j = \boldsymbol{\xi}(t_j)$ where the amplitudes of the individual components of the vector $\boldsymbol{\xi}$ might differ. Thus, network of the first type is trained on two smooth periodic one-dimensional functions – the sine wave $\mathbf{f}(t) = f(t) = \sin(2\pi t)$ and the shifted triangle wave $\mathbf{f}(t) = f(t) = 1/2 + 1/\pi \arcsin(\sin 2\pi t)$ with added noise $a_0\boldsymbol{\xi}(t)$. The time step Δt between the adjacent time points is selected equal to $\Delta t = 0.01$. The training procedure is performed for 50 epochs on the two merged sets with fixed noise amplitude a_0 having 12000 segments with 20% validation set using Adam algorithm. This way we produce individual network for each value of a_0 .

We also consider parabolic trajectories that with high accuracy resemble typical trajectories in nature describing motion of a solid object in the gravity field like a flying rock. Such trajectories are finite and essentially two dimensional. Consider a parabolic trajectory with a range b and vertex height h described by an equation $y(x) = h(1 - 4x^2/b^2)$ with $y(-b/2) = y(b/2) = 0$; the vertex $\{0, h\}$ is reached at $t = 1/2$. Assuming that points of such a trajectory are fed into a network at equal time step $\Delta t = 0.01$ one has to use a parametric representation of this curve $\mathbf{f}(t) = \{b(t - 1/2), 4ht(1 - t)\}$ where $0 \leq t \leq 1$. The noise component is also two dimensional $a_0\boldsymbol{\xi} = \{a_0\xi_x, a_0\xi_y\}$ with $a_0 = 0, 0.15, 0.4, 0.75$ and $\xi_x = 0.1\xi_y$.

A parabola can be characterized by a ratio h/b of its height h to range b . The trajectories with extreme values of this ratio $h/b \ll 1$ and $h/b \gg 1$ present cases when accurate prediction fails. When $h \ll b$ we have a very shallow trajectory and superimposed noise leads to totally random and thus unpredictable curve. For $h \gg b$ the influence of noise produces strong overlapping of ascending and descending parts of the curve that prevents good guessing of the impact point. Note here that prediction also fails when a line of sight is nearly

parallel to a plane containing a parabola – it happens mainly due to trajectory perturbations normal to that plane. For this reason, we use three parabolas with fixed value of vertex height $h = 1$ and ranges $b = 1, 2, 4$. The training procedure is performed for 50 epochs on the three merged sets with fixed noise amplitude a_0 having 18000 segments with 20% validation set using Adam algorithm.

3.2 Prediction results for one dimensional trajectories

The qualitative results are the following. The PRN trained on the data sets based on the smooth functions $f(t)$ ($a_0 = 0$) predict quite good on the similar smooth inputs when the prediction length $p \sim m$ but for $p > m$ the prediction error starts to grow. They demonstrate very low prediction ability for inputs with the noise amplitude comparable to the smooth function characteristic range (Fig. 1).

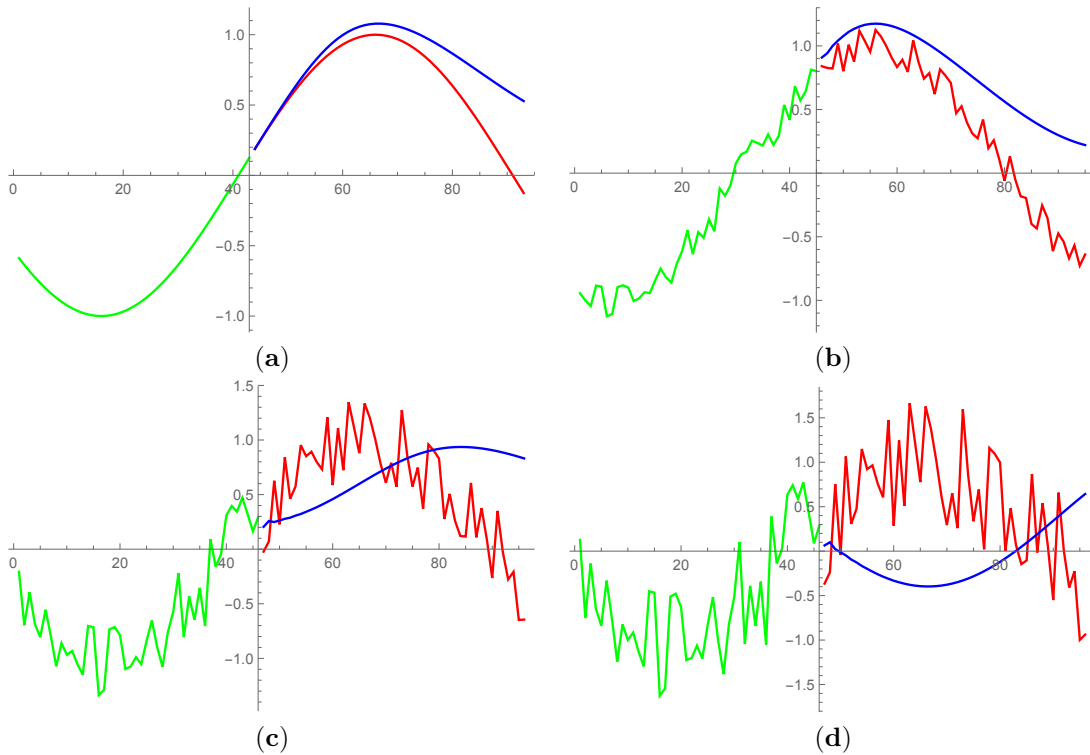


Figure 1: The input segment of a sequence (green) with (a) $a_i = 0$, (b) $a_i = 0.15$, (c) $a_i = 0.40$, (d) $a_i = 0.75$ of sine wave, the subsequent segment of the data sequence (red) and predicted dynamics (blue) by basic network with 20 neurons trained using noiseless data sets with $a_0 = 0$.

The networks trained on the noisy data sets with $a_0 > 0$ consistently fail to predict the noisy dynamics of $\mathbf{g}(t) = g(t)$, instead they produce some smooth predictions $\bar{\mathbf{g}}(t) = \bar{g}(t)$ represented by sequences $\bar{\mathbf{g}}_j = \bar{g}_j$ (few examples for $a_0 = 0.15$ are shown in Fig. 2).

It should be noted that networks with LSTM recurrent layer demonstrate better training stability and higher prediction quality compared to the ones with basic layer as shown in Fig. 3.

3.3 Prediction results for two dimensional trajectories

As in 1D case the PRN trained on the data sets based on the smooth functions fails to predict for noisy inputs. When the training data contains noise the networks appear to successfully generate quite smooth segments of all three parabolas (both ascending and descending range of curve). As shown in Fig. 4a ($a_0 = 0.15$) the prediction quality on the ascending segment improves for increasing trajectory range. On the descending segment dynamics is predicted quite well for the input noise comparable to the training noise level (Fig.

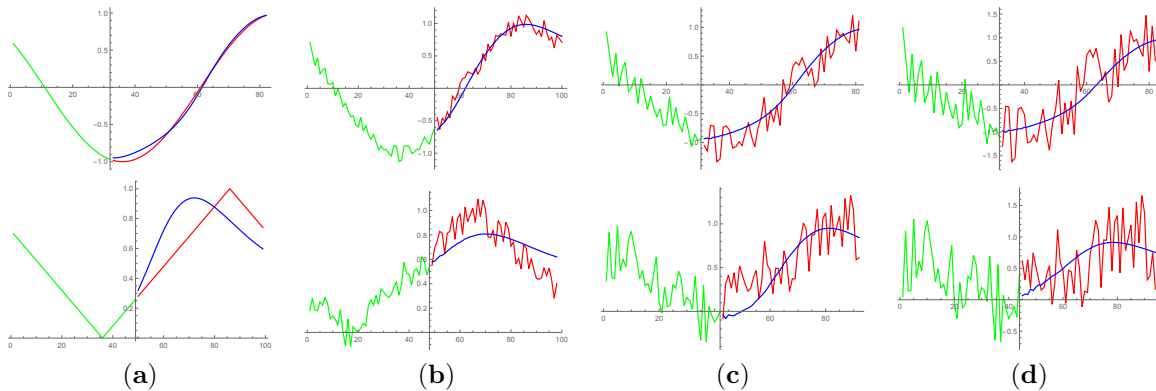


Figure 2: The input segment of a sequence (green) with (a) $a_i = 0$, (b) $a_i = 0.15$, (c) $a_i = 0.40$, (d) $a_i = 0.75$ of sine (first row) and triangle (second row) wave, the subsequent segment of the data sequence (red) and predicted dynamics (blue) using basic layer network with 20 neurons trained using data sets with noise amplitude $a_0 = 0.15$.

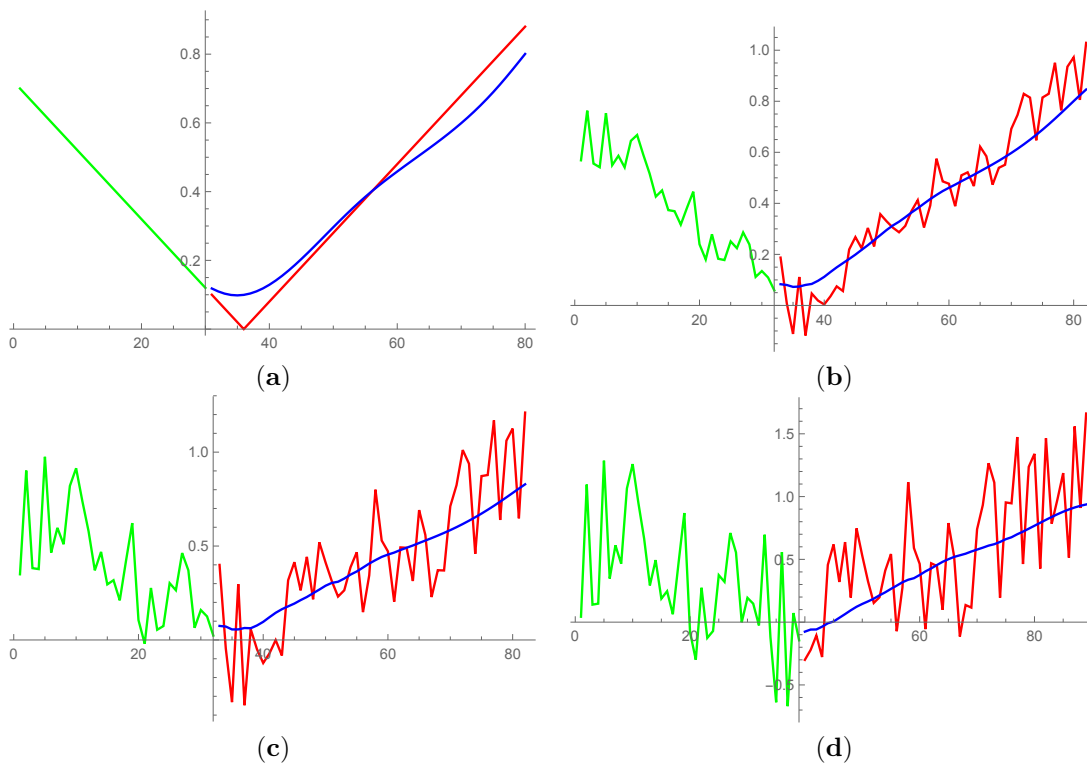


Figure 3: The input segment of a sequence (green) with (a) $a_i = 0$, (b) $a_i = 0.15$, (c) $a_i = 0.40$, (d) $a_i = 0.75$ of triangle wave, the subsequent segment of the data sequence (red) and predicted dynamics (blue) using LSTM layer network with 20 neurons trained using data sets with noise amplitude $a_0 = 0.15$.

4b,c) but for significantly larger noise the network fails to predict short and intermediate size parabolas (Fig. 4d). To remedy this weakness, we train the network for higher value $a_0 = 0.4$ of the noise component ξ and observe slight improvement of the prediction quality for large noise input (Fig. 5a).

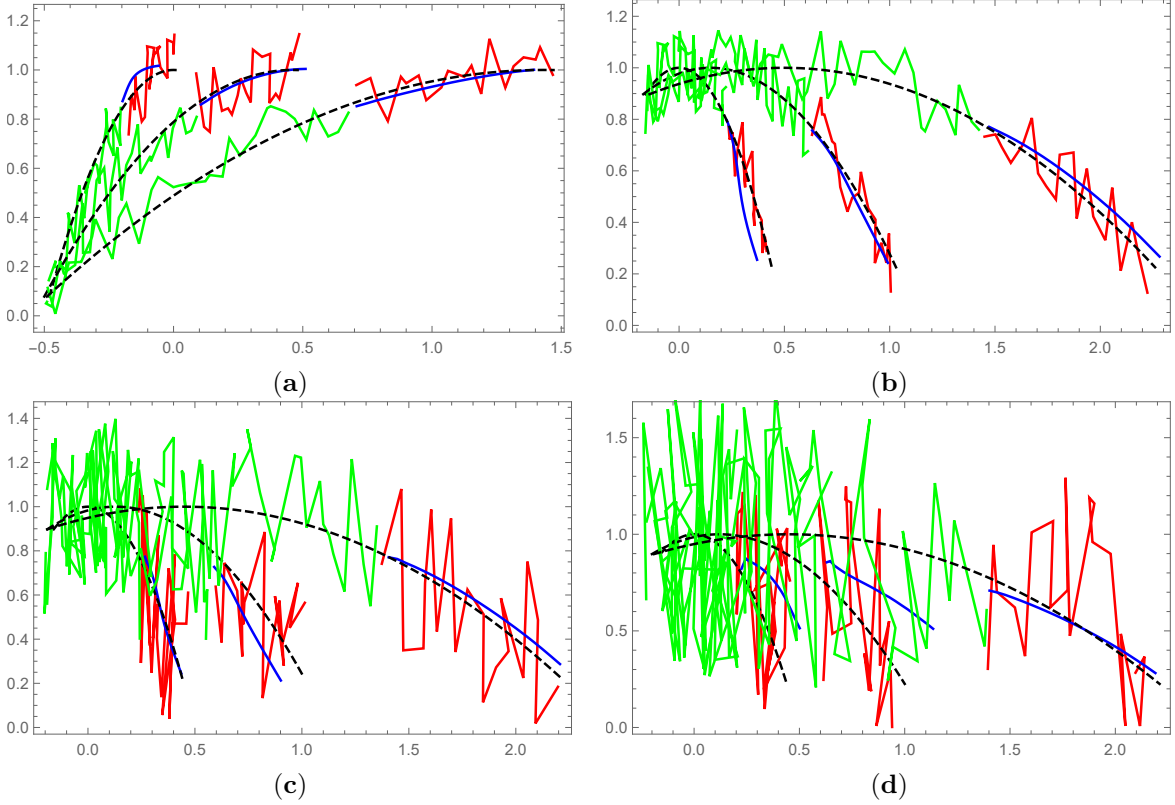


Figure 4: The input segment of a sequence (green) with (a,b) $a_i = 0.15$, (c) $a_i = 0.40$, (d) $a_i = 0.75$ of three parabolas, the subsequent segment of the data sequence (red) and predicted dynamics (blue) by LSTM layer network with 20 neurons trained on data sets with noise amplitude $a_0 = 0.15$. For comparison smooth unperturbed dynamics is shown by dashed black curve.

4 Why do noisy inputs lead to smooth predictions?

In the preceding section we consider the influence of noise in the training data as well as in the network input sequences on the network prediction and show that a trained network converts noisy input to smooth predictions. As mentioned above the numerical simulations performed in [4–6] demonstrate that the observed PRN behavior is independent of its size, architecture type as well as the predictive algorithm choice – either the “moving window”, the “expanding window” or memoryless procedure introduced in [4]. It is reasonable to assume that the smoothness of the predicted dynamics is somehow related to the training procedure.

Before turning to the training procedure analysis we consider how the noise component in the elements \mathbf{x}_i of the input sequence \mathbf{X} influences the dynamics of the network inner states \mathbf{s}_i [4].

4.1 RNN does not filter out input sequence noise component

When an input sequence $\mathbf{X} = \{\mathbf{x}_i\}$ is supplied to a network a sequence of the inner states $\mathbf{S} = \{\mathbf{s}_i\}$ is generated by recursive application of the rule (1). Consider a case of the noisy input with $\mathbf{x}_i = \mathbf{f}_i + a\boldsymbol{\xi}_i$ where a is the noise amplitude. Compute \mathbf{s}_1

$$\mathbf{s}_1 = \mathbf{F}(\mathbf{f}_1 + a\boldsymbol{\xi}_1, \mathbf{s}_0) \approx \mathbf{F}(\mathbf{f}_1, \mathbf{s}_0) + a\mathbf{J}_{x1} \cdot \boldsymbol{\xi}_1 = \hat{\mathbf{s}}_1 + a\boldsymbol{\sigma}_1,$$

where $\mathbf{J}_{x1} = \partial\mathbf{F}(\mathbf{f}_1, \mathbf{s}_0)/\partial\mathbf{x}$, and $\hat{\mathbf{s}}_1 = \mathbf{F}(\mathbf{f}_1, \mathbf{s}_0)$ is the inner state value computed for the noiseless input \mathbf{f}_1 . We observe that \mathbf{s}_1 has a noisy component proportional to the input noise amplitude a . Turn to \mathbf{s}_2 evaluation

$$\mathbf{s}_2 = \mathbf{F}(\mathbf{f}_2 + a\boldsymbol{\xi}_2, \mathbf{s}_1) = \mathbf{F}(\mathbf{f}_2 + a\boldsymbol{\xi}_2, \hat{\mathbf{s}}_1 + a\boldsymbol{\sigma}_1) \approx \mathbf{F}(\mathbf{f}_2, \hat{\mathbf{s}}_1) + a\mathbf{J}_{x2} \cdot \boldsymbol{\xi}_2 + a\mathbf{J}_{s1} \cdot \boldsymbol{\sigma}_1 = \hat{\mathbf{s}}_2 + a\boldsymbol{\sigma}_2,$$

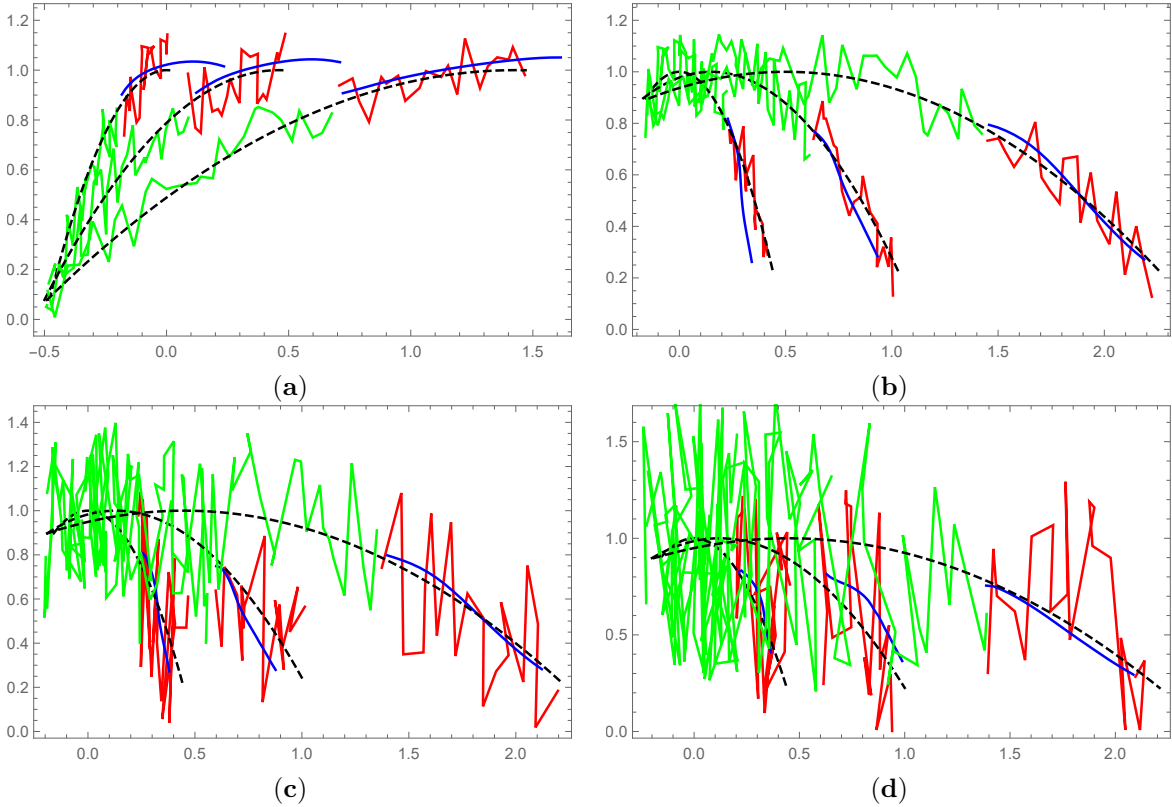


Figure 5: The input segment of a sequence (green) with (a,b) $a_i = 0.15$, (c) $a_i = 0.40$, (d) $a_i = 0.75$ of three parabolas, the subsequent segment of the data sequence (red) and predicted dynamics (blue) by LSTM layer network with 20 neurons trained on data sets with noise amplitude $a_0 = 0.4$. For comparison smooth unperturbed dynamics is shown by dashed black curve.

where $\mathbf{J}_{x_2} = \partial \mathbf{F}(\mathbf{f}_2, \hat{\mathbf{s}}_1) / \partial \mathbf{x}$, $\mathbf{J}_{s_1} = \partial \mathbf{F}(\mathbf{f}_2, \hat{\mathbf{s}}_1) / \partial \mathbf{s}$, and we obtain for the noiseless and noisy contributions to \mathbf{s}_2 the expressions

$$\hat{\mathbf{s}}_2 = \mathbf{F}(\mathbf{f}_2, \hat{\mathbf{s}}_1), \quad \boldsymbol{\sigma}_2 = \mathbf{J}_{x_2} \cdot \boldsymbol{\xi}_2 + \mathbf{J}_{s_1} \cdot \boldsymbol{\sigma}_1.$$

Repeating the procedure we obtain for $\mathbf{s}_i = \hat{\mathbf{s}}_i + a\boldsymbol{\sigma}_i$, with $\hat{\mathbf{s}}_i = \mathbf{F}(\mathbf{f}_i, \hat{\mathbf{s}}_{i-1})$, and

$$\boldsymbol{\sigma}_i = \mathbf{J}_{x_i} \cdot \boldsymbol{\xi}_i + \mathbf{J}_{s,i-1} \cdot \boldsymbol{\sigma}_{i-1}, \quad (3)$$

$$\mathbf{J}_{x_i} = \partial \mathbf{F}(\mathbf{f}_i, \hat{\mathbf{s}}_{i-1}) / \partial \mathbf{x}, \quad \mathbf{J}_{s,i-1} = \partial \mathbf{F}(\mathbf{f}_i, \hat{\mathbf{s}}_{i-1}) / \partial \mathbf{s}, \quad (4)$$

and thus demonstrate that the inner states of the network have noise component proportional to that of in the input sequence.

The dynamics of the noise component $\boldsymbol{\sigma}$ in the linear approximation defined in (3) strongly depends on the spectrum of the square matrix $\mathbf{J}_{s,i-1}$ in (4). For any square matrix \mathbf{W}_s one can find its eigenvalues λ_j ; if $|\lambda_j| < 1$ for all j the linear transformation defined by the matrix \mathbf{W}_s is contractive, i.e., $|\mathbf{W}_s \cdot \mathbf{u}| < |\mathbf{u}|$ for any vector \mathbf{u} .

Note that $\mathbf{J}_{s,i-1}$ in (4) is obtained as partial derivative of the nonlinear vector function \mathbf{F} with parameters defined in the result of PRN training and there is no guarantee that it satisfies the contraction conditions. Even if it is the case and we have $|\mathbf{J}_{s,i-1} \cdot \boldsymbol{\sigma}_{i-1}| < |\boldsymbol{\sigma}_{i-1}|$, the first term in r.h.s. of (3) cannot be neglected as $\boldsymbol{\xi}_i$ represents a *random* noise contribution to the point \mathbf{x}_i . This means that the network does not filter out noise present in the input sequence \mathbf{X} . In the multi-layer PRN the output of a given (inner) layer plays a role of the input to the next layer, so that the noise component propagates through all network layers without decay.

As the predicted value \bar{x} depends linearly on the last inner state \mathbf{s}_m one expects that the predicted value \bar{x} would also have a noisy component. It is true for an untrained network but training makes this expectation invalid. To understand this fact better we have to consider different training procedures in more details.

4.2 "Moving window" prediction procedure

Consider the "seq-to-one" training procedure with the sequences of a fixed length that corresponds to the MW prediction. Each time when the sequence of length m has the same initial point j_s the input values read $\mathbf{g}_j = \mathbf{f}_j + a_i \boldsymbol{\xi}_j, j_s \leq j \leq j_s + m$, where \mathbf{f}_j are the same but $\boldsymbol{\xi}_j$ are the random vectors with zero average. The same observation is valid for the point with $j = j_s + m + 1$ to be predicted – $\mathbf{g}_{j_s+m+1} = \mathbf{f}_{j_s+m+1} + a_i \boldsymbol{\xi}_{j_s+m+1}$. As during the training procedure this segment is used repeatedly with changing noise component the network eventually is trained to attempt prediction of an average of these points $\langle \mathbf{g}_{j_s+m+1} \rangle \approx \mathbf{f}_{j_s+m+1}$ as the noise component averages out (Fig. 6a). When the number of points n_t representing a trajectory is much smaller than the number of data sets N_d used in training procedure covering the whole trajectory, each point of the trajectory would be visited approximately $N_d/n_t \gg 1$ times and the averaging should be quite effective. As the result the training procedure for every input sequence effectively forces the network to predict *nearly all* points in a very small vicinity of the actual curve. It implies that the deviation of these points from the actual trajectory is much smaller than in the input noisy sequence and the predicted trajectory looks smooth. In other words when the original noisy sequence \mathbf{X} is supplied to the trained network the latter tries to generate the last inner state \mathbf{s}_m that is very close to its noiseless counterpart $\mathbf{s}_m \approx \hat{\mathbf{s}}_m$ (Fig. 6).

It is instructive to underline important difference between periodic (spatially infinite) and finite size trajectories represented by N points. On the latter we have one special point qualitatively different from all other points – this is the trajectory last N -th point. To predict this point, one has to use for training the segments ending at $(N - 1)$ -th point. An average number of points in such segments is smaller than n_t but the number of these segments is larger than N_d . This means that the last point is predicted with higher accuracy compared to all other points of the trajectory (Fig. 7b).

Thus the "seq-to-one" training paradigm forces a network to produce a trajectory that is close to underlying noise-free dynamics.

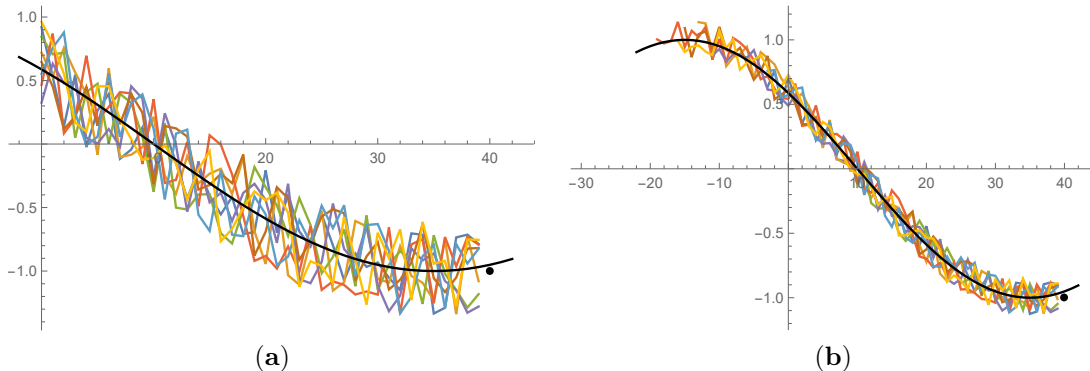


Figure 6: Averaging of the predicted point during "seq-to-one" training procedure with (a) fixed and (b) variable input sequence length. The noise amplitude of eight segments of the training data sets is $a_0 = 0.15$. Black dots denote an average of the predicted value and black solid curve represents a segment of the actual sine wave trajectory.

Consider rounds of the prediction using the memoryless algorithm that produces a predicted trajectory coinciding with that of made by the original MW algorithm.

Round 1. The input $\mathbf{X}^1 = \{\mathbf{x}_j\}, 1 \leq i \leq m$ consists of the elements of the original input sequence and has no predicted elements. As the predicted value $\bar{\mathbf{x}}^1 = \bar{\mathbf{x}}_{m+1} \approx \mathbf{f}_{m+1}$ is in the close vicinity of the actual trajectory we deduce that $\mathbf{s}_m^1 \approx \hat{\mathbf{s}}_m^1$ such that $\mathbf{f}_{m+1} = \mathbf{L}(\hat{\mathbf{s}}_m^1) = \mathbf{W} \cdot \hat{\mathbf{s}}_m^1 + \mathbf{B}$.

Round 2. For the second prediction round we form a new input $\mathbf{X}^2 = \{\mathbf{x}_2, \dots, \mathbf{x}_m, \bar{\mathbf{x}}_{m+1}\}$ and find

$$\mathbf{s}_m^2 = \mathbf{F}(\bar{\mathbf{x}}_{m+1}, \mathbf{s}_m^1) \approx \mathbf{F}(\mathbf{f}_{m+1}, \hat{\mathbf{s}}_m^1) = \hat{\mathbf{s}}_m^2.$$

Use it to predict $\bar{\mathbf{x}}_{m+2} = \mathbf{L}(\mathbf{s}_m^2) \approx \mathbf{L}(\hat{\mathbf{s}}_m^2)$ that leads to a noiseless predicted value $\bar{\mathbf{x}}_{m+2} \approx \mathbf{f}_{m+2}$.

Round 3. Repeat the above procedure to obtain $\mathbf{s}_m^3 = \mathbf{F}(\bar{\mathbf{x}}_{m+2}, \mathbf{s}_m^2) \approx \mathbf{F}(\mathbf{f}_{m+2}, \hat{\mathbf{s}}_m^2) = \hat{\mathbf{s}}_m^3$, and we again find $\bar{\mathbf{x}}_{m+3} \approx \mathbf{f}_{m+3}$.

One can see that at k -th prediction round we have

$$\mathbf{s}_m^k = \mathbf{F}(\bar{\mathbf{x}}_{m+k-1}, \mathbf{s}_m^{k-1}) \approx \mathbf{F}(\mathbf{f}_{m+k-1}, \hat{\mathbf{s}}_m^{k-1}) = \hat{\mathbf{s}}_m^k, \quad \bar{\mathbf{x}}_{m+k} \approx \mathbf{f}_{m+k}. \quad (5)$$

4.3 "Expanding window" prediction procedure

Now turn to the training procedure using segments of variable length corresponds to the EW prediction. Consider all training segments having the last point $\mathbf{g}_{j_s+m} = \mathbf{f}_{j_s+m} + a_i \boldsymbol{\xi}_{j_s+m}$. The point for the prediction for all such segments has $j = j_s + m + 1$. As we note above the noise component of all these points should average out and it again predicts $\langle \mathbf{g}_{j_s+m+1} \rangle \approx \mathbf{f}_{j_s+m+1}$. (Fig. 6b, 7).

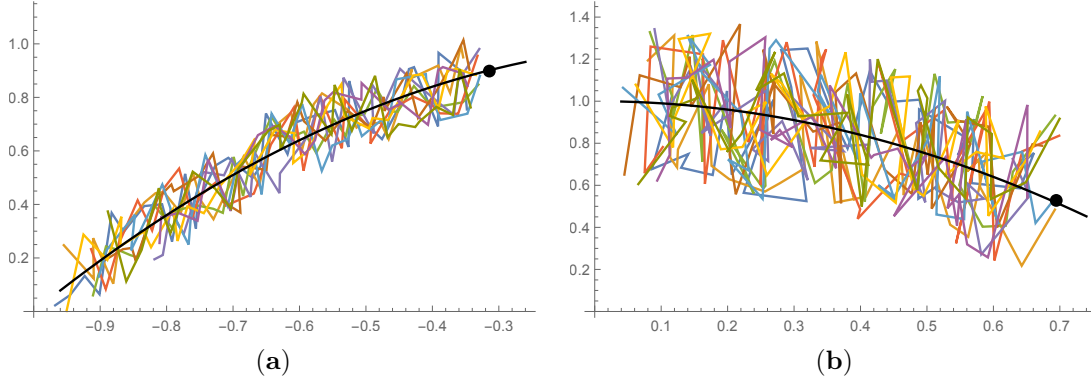


Figure 7: Averaging of the predicted point during "seq-to-one" training procedure with variable input sequence length in the (a) ascending and (b) descending segment of parabolic trajectory. The number and noise amplitude of the training segments is (a) 10 segments with $a_0 = 0.15$ and (b) 20 segments with $a_0 = 0.4$. Black dots denote an average of the predicted value and black solid curve represents the actual trajectory segment.

Round 1. The input $\mathbf{X}^1 = \{\mathbf{x}_j\}$, $1 \leq i \leq m$ consists of the elements of the original input sequence and has no predicted elements. As the predicted value $\bar{\mathbf{x}}^1 = \bar{\mathbf{x}}_{m+1} \approx \mathbf{f}_{m+1}$ is in the close vicinity of the actual trajectory we deduce that $\mathbf{s}_m^1 \approx \hat{\mathbf{s}}_m^1$ such that $\mathbf{f}_{m+1} = \mathbf{L}(\hat{\mathbf{s}}_m^1) = \mathbf{W} \cdot \hat{\mathbf{s}}_m^1 + \mathbf{B}$.

Round 2. For the second prediction round we have to form a new input \mathbf{X}^2 with $m + 1$ elements by adding the predicted value $\bar{\mathbf{x}}_{m+1}$ to \mathbf{X}^1 and producing $\mathbf{X}^2 = \{\mathbf{x}_1, \mathbf{x}_2, \dots, \mathbf{x}_m, \bar{\mathbf{x}}_{m+1}\}$. Note that the last element of \mathbf{X}^2 has much lower noise amplitude compared to all preceding terms. Feeding this sequence into the network we produce a sequence of the inner states \mathbf{s}_i^2 using (1) as $\mathbf{s}_i^2 = \mathbf{F}(\mathbf{x}_i^2, \mathbf{s}_{i-1}^2)$. Evaluate the last term $\mathbf{s}_{m+1}^2 = \mathbf{F}(\mathbf{x}_{m+1}^2, \mathbf{s}_m^2)$ and note that $\mathbf{x}_{m+1}^2 = \bar{\mathbf{x}}_{m+1} \approx \mathbf{f}_{m+1}$. As $\mathbf{s}_m^2 \approx \hat{\mathbf{s}}_m^1$ we find both arguments of \mathbf{F} correspond to noiseless values leading to

$$\mathbf{s}_{m+1}^2 \approx \mathbf{F}(\mathbf{f}_{m+1}, \hat{\mathbf{s}}_m^1) = \hat{\mathbf{s}}_{m+1}, \quad \bar{\mathbf{x}}_{m+2} = \mathbf{L}(\mathbf{s}_{m+1}^2) \approx \mathbf{f}_{m+2}.$$

and the predicted value $\bar{\mathbf{x}}_{m+2}$ is also close to the actual trajectory.

Round 3. In the next round we create an input \mathbf{X}^3 with two last values $\mathbf{x}_{m+2}^3 \approx \mathbf{f}_{m+2}$ and $\mathbf{x}_{m+1}^3 \approx \mathbf{f}_{m+1}$ close to the actual trajectory. We have $\mathbf{s}_{m+1}^3 \approx \hat{\mathbf{s}}_{m+1}$ so that $\mathbf{s}_{m+2}^3 = \mathbf{F}(\mathbf{x}_{m+2}^3, \mathbf{s}_{m+1}^3) \approx \mathbf{F}(\mathbf{f}_{m+2}, \hat{\mathbf{s}}_{m+1}) = \hat{\mathbf{s}}_{m+2}$ and we obtain $\bar{\mathbf{x}}_{m+3} = \mathbf{L}(\mathbf{s}_{m+2}^3) \approx \mathbf{f}_{m+3}$.

Repeating the prediction rounds in similar manner we arrive at the general k -th term of the predicted sequence

$$\mathbf{s}_{m+k-1}^k = \mathbf{F}(\mathbf{x}_{m+k-1}^k, \mathbf{s}_{m+k-2}^k) \approx \mathbf{F}(\mathbf{f}_{m+k-1}, \hat{\mathbf{s}}_{m+k-2}) = \hat{\mathbf{s}}_{m+k-1}, \quad \bar{\mathbf{x}}_{m+k} = \mathbf{L}(\mathbf{s}_{m+k-1}^k) \approx \mathbf{f}_{m+k}. \quad (6)$$

The results (5,6) demonstrate that both a sequence of the predicted values $\bar{\mathbf{x}}_{m+k}$ and a sequence of the corresponding network inner states \mathbf{s}_m^k represent smooth trajectories in their respective phase space.

5 Recurrent network architecture generalizations

In the preceding sections we consider simple PRN with inner dynamics described by (1) trained to predict a single point of trajectory (“seq-to-one” networks) that follows the input sequence. We demonstrate and explain an unexpected ability of such networks being well trained on noisy sequences representing an apparent trajectory to predict actual smooth trajectory. It is instructive to verify whether this property persists in networks with more general architectures, namely “seq-to-seq” networks.

“Seq-to-seq” architecture uses the input sequence of fixed or variable length while the predicted sequence has a fixed length $l > 1$. It uses a training procedure [7] with the last element s_m of the inner state sequence copied p times and this new sequence is submitted to another PRN that eventually generates the desired output sequence $\{\bar{x}_{m+j}\}$, $1 \leq j \leq l$. During the training all predicted sequences having the same initial point or those that overlap significantly contribute to averaging that effectively allows to predict the fixed size segment of the trajectory close to the actual one. As the complete overlapping of the predicted segments is relatively rare the prediction curve smoothness is expected to be lower than in case of the “seq-to-one” training algorithm (Fig. 8a). It is confirmed by numerical simulations in [6] of prediction of phase modulated

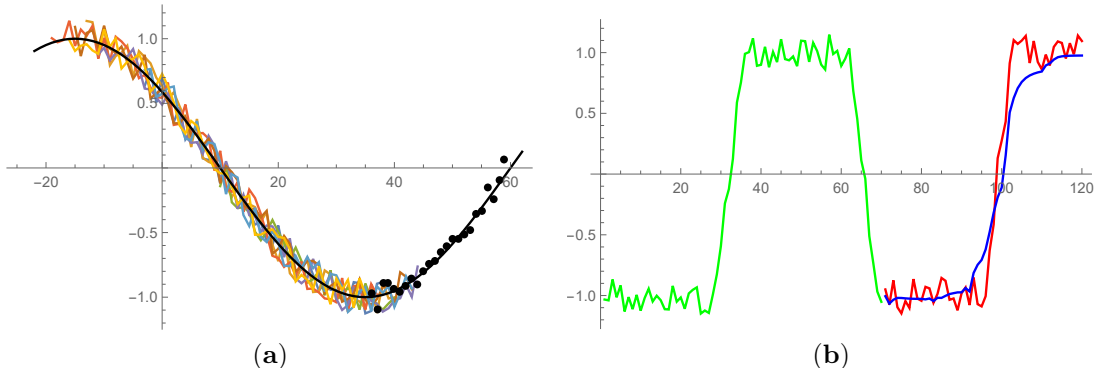


Figure 8: (a) Averaging of the predicted points for “seq-to-seq” training with variable input. The noise amplitude of eight segments of the training data sets is $a_0 = 0.15$. Black dots denote an average of $l = 15$ values in the predicted sequence and black solid curve represents a segment of the actual sine wave trajectory. (b) Comparison of the ground truth continuation (red) of the input noisy phase modulated trapezoid wave sequence (green) to the predictions computed by MW algorithm (solid blue) in the network with the total number of neurons $n = 50$. The length of the input sequence $m = 70$ and the predicted sequence size is $kl = 40$ with $l = 10$.

trapezoid wave (Fig. 8b) that also shows that the “roughness” of the predicted curve is still smaller than that of the input sequence.

6 Noiseless prediction of time series in biology context

In our opinion the “built-in” ability of RNNs to generate smooth prediction dynamics plays very important role in biological evolution of mobile organisms. Any mobile organism that receives and processes information about position and dynamics of other moving objects and immobile obstacles in its vicinity should be able at least to avoid collisions with these objects to increase its survival probability. To this end the organism should have an ability to predict trajectories in space. In most cases actual trajectories have negligible low noise amplitude but the corresponding apparent ones processed by the organism predictive network might have much higher noise levels. The origin of this noise includes motion of the organism itself and errors in the sensors detecting trajectories.

It is important to underline that ubiquity of noisy sequences encoding smooth trajectories forces PRNs to learn to predict based on noisy input data sets. The same time it is reasonable to assume that the organism *has to predict* the actual smooth trajectory – if otherwise a noisy trajectory is predicted the error of prediction would be too large in order to generate a required reaction of the organism. It looks impossible to resolve the

apparent contradiction between a perturbed noisy input trajectory and a desired smooth predicted dynamics that emerges in biological context. But it appears that this requirement is satisfied nearly automatically as a default feature of PRNs of sufficient size trained on the noisy data sets that arise *naturally* in biology.

Turning to prediction of specific trajectory types we start with computationally preferable infinite one-dimensional periodic sine and triangle waves. The simulations confirm that indeed PRNs trained on noisy datasets successfully predict basic smooth curves. Unfortunately, perfectly periodic in space and time trajectories are nearly absent in nature. Instead finite trajectories are omnipresent and thus their prediction is important for survival. One class of such trajectories includes parabola describing with high accuracy passive motion of a (small) solid object under gravity force. The prediction of an ascending segment of parabola is a valuable trait for getting fruit hanging from a tree. The same time accurate guess of the final segment of a descending tail of parabola is important to evade being hit by a flying object.

The parabola has two important parameters – the maximal height h and the range (distance between the initial and end points) b , their ratio h/b is critical for prediction process. Essentially we argue that both extreme cases $h/b \ll 1$ and $h/b \gg 1$ represent curves that nearly impossible to predict. We choose three parabolas with $h/b = 1, 1/2, 1/4$ and fixed $h = 1$ as typical examples of predictable trajectories and trained PRNs designed to "recognize" and reproduce all three curves. We show that for noisy input sequence representing these essentially two-dimensional curves PRNs can predict smooth continuation that follows the unperturbed path of a moving object.

The main result of this manuscript also may be applicable in more general context of biological evolution. This evolution is viewed as a process of learning by a network that tries to predict dynamics of the environment [9]. In this approach an organism fitness increases when it can successfully predict the environment variables dynamics, *i.e.*, when the predictive error (a loss function) reaches a (local) minimum. Taking into account that the environment variables have an inherent noisy component and the organism receptors sense these variables with some error one has to deduce that the training data sets are always noisy ($a_0 > 0$). The same time it is desirable to be able to predict a trend of the environment changes. Thus, we again encounter the same problem of predicting smooth dynamics based on the input sequences with nonzero noise amplitude, and the problem is solved due to unexpected "predictive smoothing" feature of trained PRNs.

7 Discussion

A traditional approach of predicting neural networks holds that a trained network is expected to predict time series with the same qualitative features as those characterizing the input data. This view can be justified when the input signal to the network is smooth, *i.e.*, when the input signal has the same noise level as the actual trajectory and the network is trained on such signals $a_0 = a_i = 0$. When the input signal is noisy and the network trained on the smooth signal ($a_i > a_0 = 0$), it fails to predict with reasonable accuracy.

Thus the paradigm should be changed to one that allows both the training data sets and input signals have nonzero noise component $a_0, a_i > 0$ reflecting real case scenario. The numerical experiments presented above demonstrate that PRNs trained with noisy data sets ($a_0 > 0$) predict smooth trajectories for both smooth ($a_i = 0$) and perturbed ($a_i > 0$) inputs. When the number of neurons is large enough the predicted trajectories appear to be quite close to the actual trajectories $\mathbf{f}(t)$. We argue that prediction of smooth trajectories is mainly due to the training procedures but it also can be related to predictive algorithm choice.

The application of both MW and EW predictive algorithms as well as their memoryless counterparts for the trained PRN with sufficient number of neurons would produce a sequence of points that are positioned close to the actual trajectory $\mathbf{f}(t)$. The statistical arguments used in the manuscript allow to explain "smoothness" of the predicted dynamics for the well trained networks. It might happen that this is not the only reason for such a behavior and the actual explanation requires much deeper insight into mathematical facet of the problem.

This statement is based on the following observation – it was reported in [4] that a *trained* PRN with a small number of neurons that cannot successfully predict an actual trajectory still generates a *smooth* curve. The same time preliminary numerical experiments show that on the contrary *untrained* PRNs with randomly set trainable parameters demonstrate periodic and even chaotic transient behavior as well as stable periodic long time predicted dynamics. One can view that as a mathematical curiosity which is irrelevant from the biological point of view as a low prediction quality diminishes survival probability that creates an evolutionary

pressure forcing an organism to increase the size (number of neurons) of predictive network.

What is the difference between the trained and untrained network? From the mathematical perspective PRNs dynamics is governed by a discrete time map (A4) with the corresponding set of parameters. Random parameters of the untrained network in a process of training are replaced by another set for the trained network. As we observe the training "forces" a network to generate the first point of the predicted trajectory to be in a small vicinity of the unperturbed trajectory. On the contrary, the corresponding point produced by an untrained PRN lies much further off the actual curve. The consecutive steps of prediction by EW algorithm depend on the inner dynamical properties of the map (A4).

This fact illuminates two-sided effect of a training procedure. First, its main goal is to produce a proper location of a single predicted point in "seq-to-one" paradigm. Additionally the same training process gives rise to a specific discrete time map (A4) that determines recursively predicted dynamics beyond the first point. Number of qualitatively different predicted trajectories depends only on the nonlinear map (A4) while the selection between them is due to position of the first predicted point (mostly determined by the input sequence). In the framework of dynamical system theory different trajectories correspond to different attractors of (A4) each one having its unique basin of attraction. The number of attractors and complexity of the basin topology usually grows with increase in number of parameters (network size).

When the number of neurons is small the trajectories are very simple, e.g., smooth approach to a steady state point and the network fails to reproduce a desired dynamics. If even such unsuccessful training leads to generation of some smooth dynamics by (A4) then this property might be a main reason for smooth prediction made by well trained PRNs and it deserves separate investigation.

In this manuscript we consider how perturbations of input sequences affect robustness of predictions made by PRNs trained with data sets of various noise level. In other words, we investigate how an external perturbation influences the network performance. It would be instructive to consider results of trained network internal perturbation effected by disabling of one or more neurons. From the neuroscience perspective such a scenario is quite possible in natural neural networks. In more relevant problem formulation when a network consists of several recurrent layers this question becomes more complex as one might expect that damage of a few neurons in the inner layers would have less effect on the prediction quality compared to switching the neurons off in the first or last layer. Investigation of multilayer predictive network dynamics will be published elsewhere.

Appendix

Memoryless vs. EW/MW prediction algorithm

The first prediction round of the algorithm is the same as in MW/EW algorithms – a sequence \mathbf{X}^1 of length m is fed into the network that produces \mathbf{s}_m^1 to generate the prediction $\bar{\mathbf{x}}_{m+1} = \mathbf{L}(\mathbf{s}_m^1)$.

In regular EW algorithm for the second round one forms a new expanded sequence \mathbf{X}^2 of length m $\mathbf{X}^2 = \{\mathbf{x}_1, \mathbf{x}_2, \dots, \mathbf{x}_m, \bar{\mathbf{x}}_{m+1}\}$ and feeds it into the network to produce

$$\mathbf{s}_{m+1}^2 = \mathbf{F}(\mathbf{x}_{m+1}^2, \mathbf{s}_m^2) = \mathbf{F}(\bar{\mathbf{x}}_{m+1}, \mathbf{s}_m^1). \quad (\text{A1})$$

Here we use the facts that $\mathbf{x}_{m+1}^2 = \bar{\mathbf{x}}_{m+1}$ and $\mathbf{s}_m^2 = \mathbf{s}_m^1$ as the first m elements in \mathbf{X}^1 and \mathbf{X}^2 coincide. We observe that both arguments in $\mathbf{F}(\bar{\mathbf{x}}_{m+1}, \mathbf{s}_m^1)$ are found at the first prediction round. Thus we can retain the inner state \mathbf{s}_m^1 as the current state of the network and use the prediction $\bar{\mathbf{x}}_{m+1}$ as an input to RNN to compute \mathbf{s}_{m+1}^2 and to arrive at $\bar{\mathbf{x}}_{m+2} = \mathbf{L}(\mathbf{s}_{m+1}^2)$.

In the third round we have $\mathbf{X}^3 = \{\mathbf{x}_1, \mathbf{x}_2, \dots, \mathbf{x}_m, \bar{\mathbf{x}}_{m+1}, \bar{\mathbf{x}}_{m+2}\}$ and obtain

$$\mathbf{s}_{m+2}^3 = \mathbf{F}(\mathbf{x}_{m+2}^3, \mathbf{s}_{m+1}^3) = \mathbf{F}(\bar{\mathbf{x}}_{m+2}, \mathbf{s}_{m+1}^2) = \mathbf{F}(\mathbf{L}(\mathbf{s}_{m+1}^2), \mathbf{s}_{m+1}^2), \quad \bar{\mathbf{x}}_{m+3} = \mathbf{L}(\mathbf{s}_{m+2}^3). \quad (\text{A2})$$

Continue the same procedure into k -th prediction round to find

$$\mathbf{s}_{m+k-1}^k = \mathbf{F}(\mathbf{x}_{m+k-1}^k, \mathbf{s}_{m+k-2}^k) = \mathbf{F}(\bar{\mathbf{x}}_{m+k-1}, \mathbf{s}_{m+k-2}^{k-1}) = \mathbf{F}(\mathbf{L}(\mathbf{s}_{m+k-2}^{k-1}), \mathbf{s}_{m+k-2}^{k-1}), \quad (\text{A3})$$

We observe that the results generated by the EW approach can be obtained with its ML version that does not require repeated construction of the input sequences of increasing length.

Note that the last element of the inner state sequence at the round k reads \mathbf{s}_{m+k-1}^k and the superscript k might be dropped. Rewrite (A3) as

$$\mathbf{s}_{m+k-1} = \mathbf{F}(\bar{\mathbf{x}}_{m+k-1}, \mathbf{s}_{m+k-2}) = \mathbf{F}(\mathbf{L}(\mathbf{s}_{m+k-2}), \mathbf{s}_{m+k-2}) = \mathbf{H}(\mathbf{s}_{m+k-2}), \quad (\text{A4})$$

that represents a vector discrete map transforming the last state \mathbf{s}_{m+k-2} of the input sequence \mathbf{X}^{k-1} into a similar term \mathbf{s}_{m+k-1} in the next predictive round. As soon as the first prediction round is over and the value \mathbf{s}_m is computed the predicted sequence can be obtained as the result of recurrent application of the map (A4) to \mathbf{s}_m . In other words, the prediction is determined by the *autonomous* dynamics of the network. It should be underlined here that if the network is untrained or when the number of neurons is too small to make a reliable prediction the map (A3) will generate the same sequence due to EW approach.

Considering the "moving window" algorithm first note that if the network is well trained, *i.e.*, the predicted value is close to the actual trajectory then EW version is preferable over MW approach as it uses the larger input sequences. In such a case one expects that the predictions of these two algorithms should not differ significantly and thus the ML algorithm can be used too. Moreover, the numerical experiments performed with untrained and small size networks that do not demonstrate high predictive quality show that both MW and EW (ML) algorithms still generate predicted sequences that are very close to each other.

References

- [1] S. Haykin (Ed.), *Kalman filtering and neural networks*, John Wiley, 2001.
- [2] K. Yeo, Short note on the behavior of recurrent neural network for noisy dynamical system, 2019, [arXiv:1904.05158 \[cs.NE\]](#).
- [3] S. Hochreiter, J. Schmidhuber, Long-short term memory, *Neural Comput.*, 1997, **9**, 1735-1780.
- [4] B. Rubinstein, A fast noise filtering algorithm for time series prediction using recurrent neural networks, 2020, [arXiv:2007.08063v3 \[cs.LG\]](#).
- [5] B. Rubinstein, A fast memoryless predictive algorithm in a chain of recurrent neural networks, 2020, [arXiv:2010.02115v1 \[math.DS\]](#).
- [6] B. Rubinstein, On a novel training algorithm for sequence-to-sequence predictive recurrent networks, 2021, [arXiv:2106.14120v1 \[cs.LG\]](#).
- [7] I. Sutskever, O. Vinyals, Q.V. Le, Sequence to sequence learning with neural networks, 2014, [arXiv:1409.3215v3 \[cs.CL\]](#).
- [8] T.B. Brown, B. Mann et al., Language Models are Few-Shot Learners, 2020, [arXiv:2005.14165v4 \[cs.CL\]](#).
- [9] V. Vanchurin, Y.I. Wolf, M.I. Katsnelson, E.V. Koonin, Toward a theory of evolution as multilevel learning, *PNAS*, 2022, **119**, e2120037119.